ATTACHMENT A

ELSEVIER

Polymer 42 (2001) 1953–1967

polymer

www.elsevier.nl/locate/polymer

Characterization of the molecular structure of two highly isotactic polypropylenes

P. Viville[a], D. Daoust[a,*], A.M. Jonas[a], B. Nysten[a], R. Legras[a], M. Dupire[b], J. Michel[b], G. Debras[b]

[a]*Faculté des Sciences Appliquées, Unité de Physique et de Chimie des Hauts Polymères, Université Catholique de Louvain, Bâtiment Boltzmann, Place Croix du Sud, 1 B-1348 Louvain-la-Neuve, Belgium*

[b]*FINA RESEARCH S.A — Zone Industrielle C, 7181 Seneffe, Belgium*

Received 5 April 2000; received in revised form 15 May 2000; accepted 13 June 2000

Abstract

Two polypropylenes, PP_1 and PP_2, produced with different heterogeneous Ziegler–Natta catalytic systems were studied in this work. Preliminary characterization of the non-fractionated materials showed that a low difference in their average tacticity ($PP_2 > PP_1$) leads to an important modification of their rigidity properties. In order to establish correlation between the molecular structure parameters and the rigidity properties of these polymers, fractionation of the materials according to crystallizability was performed by means of temperature rising elution fractionation (TREF). Analysis of the fractions of both PP_1 and PP_2 was carried out by means of ^{13}C NMR, size exclusion chromatography (SEC), differential scanning calorimetry (DSC) and atomic force microscopy (AFM). The results first showed that TREF does not strictly fractionate PP according to tacticity, but according to the longest crystallizable sequence in a chain. ^{13}C NMR, SEC and DSC analysis of the fractions demonstrated that the inter-chain tacticity distributions of the polypropylenes is affected by the change of the polymerization conditions, which, in turn, modifies the rigidity properties of the materials. Some results also seem to indicate that the intra-chain tacticity distributions are different for the two PP. An AFM study of the elastic modulus was carried out for the first time on the TREF fractions. It showed that the rigidity of the fractions strongly increases as the TREF elution temperature increases in accordance with a concomitant increase of isotacticity and the crytallinity of the fractions. PP_2 TREF fractions were, moreover, found to exhibit a higher elastic modulus than PP_1 TREF fractions at all elution temperatures. This study allowed us to further identify the TREF fractions that were responsible for differences in rigidity. To summarize, it is shown how the experimentally observed increase of the average rigidity of one of these two polypropylenes can be rationalized via information collected from a TREF fractionation. © 2000 Published by Elsevier Science Ltd.

Keywords: Temperature rising elution fractionation; Polypropylene; Molecular structure

1. Introduction

Polyolefins are today among the most important commodity polymers. More precisely, polyethylenes and polypropylenes are the major tonnage of plastic materials worldwide. The reason why these two polymers have attracted so much interest is mainly the diversity of structural variants that one can obtain by the use of ethylene and propylene monomers through the use of Ziegler–Natta catalysts, discovered in the early 1950s, and appropriated polymerization processes. Indeed, Ziegler–Natta catalysts have evolved considerably from the low active, low stereospecific catalysts to the highly active, highly stereospecific catalysts used in modern polyolefin manufacturing plants. Today, highly efficient Ziegler–Natta catalysts and new process technologies lead to a very broad range of applications and polyolefins can now span the full range of polymeric properties from soft elastomers to hard thermoplastics, depending on the relative composition of ethylene and propylene and the manner of their enchainment [1–3].

One important issue in the field of polyolefins is the control of their rigidity. One example for which this issue is of considerable industrial relevance is the case of toughened polypropylenes PP/EP [3]. Indeed, polypropylene itself has excellent physical properties, such as high stiffness and tensile strength. However, it has poor impact strength and is very brittle at low temperatures, which limits its applications. When ethylene–propylene rubber (EPR) is added to polypropylene as minor component, an improvement of impact strength is observed and the brittleness temperature is decreased [3–5]. The actual trend of the market is to enhance the rigidity of these materials while retaining their impact strength properties. This aim can be

* Corresponding author.

0032-3861/01/$ - see front matter © 2000 Published by Elsevier Science Ltd.
PII: S0032-3861(00)00529-2

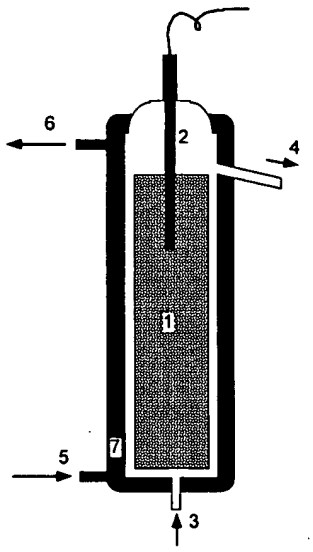

Fig. 1. Schematic view of the preparative TREF column.

achieved, for instance, by enhancing the tacticity of the polypropylene homopolymer phase and thus its crystallinity and rigidity. This is typically realized via a proper modification of the Ziegler–Natta catalytic system, which tends to decrease the amount of stereodefects on the polypropylene chains.

Although there are many different types of heterogeneous Ziegler–Natta catalysts, most have a common intriguing characteristic; they yield polymers with broad molecular mass distribution (MMD) and, in the case of copolymerization, broad chemical composition distribution (CCD) [1,2,6]. In that context, a modification of the catalyst is expected to fundamentally modify the molecular structural features of the polypropylene such as its MMD and the tacticity distribution with respect to the different molecular masses, which is believed to have a significant impact on polymer properties [7,9]. It is now fully accepted that these broad distributions are due to the presence of multiple active sites in heterogeneous catalysts [1,6,8,9]. The complexity of active sites has prevented their thorough study, challenging many researchers. It was impossible to synthesize single Ziegler–Natta catalysts. From the fine characterization of the molecular structure (or architecture), indirect information can be gained on active sites and the polymerization mechanisms could also be inferred. Literature reports many works aiming to control the tacticity index through adequate choice of external and internal electron donors. The reduction of the number of tacticity defects in the polymer chain results in a significant increase of the stiffness [9–11]. Although modification of the catalysis is suspected to modify the molecular structure of polypropylenes in terms of both inter-chain and intra-chain tacticity distribution, no clear experimental evidence of this effect has been reported up to now. These aspects are, however, of considerable interest for the understanding of the effect of the catalysis modification on the final rigidity properties.

This paper reports correlation between the molecular structure and the rigidity of two polypropylenes (PP_1 and PP_2) synthesized via different polymerization conditions and characterized by different stiffness. In order to reach this goal, a complete description of the molecular structure of the two polymers must be obtained. Since macroscopic properties of polymers cannot be uniquely determined by average values, a fractionation approach is adopted in this work. To separate polymers produced with different active sites, a number of methods described in the literature have been employed, including solvent-extraction, consecutive extraction with different solvents, fractionation with solvent/non-solvent pairs, consecutive extraction with a solvent at different temperatures [11–14], and more recently, temperature rising elution fractionation (TREF) [8–10,15]. Preparative TREF provides a much more powerful tool than do other methods, because the temperature for fractionation can be freely selected within a certain range. Moreover, it fractionates polymers on the basis of their crystallizability, and the TREF data directly reflects the tacticity of polypropylene [8–10,15,16]. In this context, TREF has gained increasing popularity over the past few years. In the literature, TREF has been mainly used as a powerful tool to probe a qualitative tacticity distribution along with a modification of the nature of the catalysis [1,9,10,16].

In the present study, we used preparative TREF as a primary technique to separate the PP complex mixtures into different fractions with respect to their different crystallizability. These fractions are then individually studied in order to characterize their molecular structure and their physical properties by means of ^{13}C NMR, size exclusion chromatography (SEC), differential scanning calorimetry (DSC) and atomic force microscopy (AFM). Based on the comparison between the two polypropylene fractionations, analysis of the molecular structure and the physical properties of fractions of the two polypropylenes is expected to yield information on the influence of the catalysis modification on both the inter-molecular and the intra-molecular heterogeneity of the polymers, respectively, corresponding to the inter-chain and intra-chain distribution of the tacticity. Emphasis is placed here on the relationship between the molecular structure of the fractions and the final rigidity of the whole material.

2. Experimental section

2.1. Materials

Materials studied in this work were two highly isotactic polypropylene homopolymers, namely PP_1 and PP_2, obtained through traditional heterogeneous Ziegler–Natta catalysis. The polymerization conditions were here properly tuned in order to increase the rigidity of PP_2. These materials obtained in a "fluff" form were stabilized with Irganox

1010 antioxidant (1500 ppm) using the Slurry method (acetone containing the required amounts of antioxidant was poured on the fluff in a beaker and the resulting slurry was stirred. Acetone was then removed from the fluff in a vacuum oven at 50°C).

2.2. Characterization

2.2.1. Preparative temperature rising elution fractionation

Complete descriptions of the TREF procedure have already been given in earlier publications [8–10,15]. In this work, a home-made preparative TREF apparatus was used. It is schematically described in Fig. 1. It consists of a double-tube glass column packed with a stainless steel wire-mesh support (*part 1*) (type "multiknit", specific weight = 525 g/dm^3, exchange surface = 215 dm^2/dm^3). The temperature of the column is controlled using a temperature controller consisting of a silicon oil bath, circulating the oil through the outer tube of the column (*parts 5, 6 and 7*), equipped with a thermostat (JULABO-MT4). A thermal probe inserted in the top of the column allows us to measure the temperature inside the column (*part 2*). For the elution of the different fractions, the column is connected to a system through which the solvent was pumped (Water 510 pump) at a flow rate of 10 ml/min (*parts 3 and 4*).

Operational conditions are described in what follows. 6 g of fluff (impregnated with antioxidant) were introduced in a 1000-ml flask containing 300 ml of xylene stabilized with 1100 ppm Irganox 1010. The polymer was dissolved at 130°C for about 30 min. The hot polymer solution was then loaded into the inner part of the glass column, the temperature of the column being initially fixed at 130°C. During the first step of the fractionation, namely the precipitation step, the solution was allowed to cool to room temperature at a rate of 0.04°C/min from 130 to 30°C. After cooling, fractions of the polymer with increasing crystallinity were then eluted with xylene at temperatures increasing stepwise. Extraction took place over temperatures ranging from 30 to 130°C divided into 17 steps (30, 40, 50, 60, 70, 80, 90, 100, 103, 106, 109, 112, 115, 118, 121, 124 and 130°C). Polymer was eluted during 120 min at every step after the temperature had stabilized for 30 min. Fractions were then collected and precipitated in methanol stabilized with Irganox 1010 under stirring, filtrated on PTFE 0.5-μm filters (Millipore, type FH 0.5), and finally dried in a vacuum oven at 50°C.

2.2.2. Differential scanning calorimetry

All the DSC runs were recorded on a DSC 821e/700 METTLER TOLEDO Differential Scanning Calorimeter. DSC runs of both global samples and of TREF fractionated samples were carried out under the following conditions: (1) a premelting of the samples was performed during a first heating to 200°C in order to standardize their thermal history (the samples were left for 5 min at 200°C); (2) cooling from 200 to −30°C at a rate of 10°C/min; and (3) a second heating from −30 to 200°C at a rate of 10°C/min. All the measurements were performed in a nitrogen atmosphere. The samples (about 5–10 mg) were enclosed in standard 40-μl aluminum pans. The temperature calibration was realized using indium (m.p. 156.6°C) and lead (m.p. 327.5°C). In both crystallization and melting experiments, the peak temperatures and corresponding enthalpies were detected.

2.2.3. Dynamic mechanical analyses

Elastic modulus (E') at 25°C and temperature dependence of the viscoelastic properties of the non-fractionated PP were determined from DMA analysis according to a three-point bending solicitation mode (RSA II mechanical spectrometer from Rheometrics, Inc.). Experimental parameters were: frequency = 1 Hz, strain amplitude = 0.02%. Measurements were carried out on samples whose dimensions were (50 × 10) mm^2 × 2 mm. For this purpose, stabilized polymer fluffs were compression molded between hot plates at 200°C under a clamping force of 10 tons for 2 min (pressure: 10^5/surface in Pa), crystallized at 100°C under 10 T for 1 min and allowed to cool at room temperature.

2.2.4. Size exclusion chromatography

The molecular mass averages and molecular mass distributions (M_w, M_n, and MMDs) of the initial samples and their TREF fractions were measured with a Waters-Millipore SEC instrument model ALC/GPC 150C equipped with a differential refractometer detector (DRI). The following operational conditions were adopted. Solutions of the polymer were prepared by dissolving the material in 1,2,4-trichlorobenzene (TCB) stabilized with antioxidant Irganox 1010 at a concentration of 2 g/l. Dissolution was allowed for 1 h at 160°C. 120 μl of the solution was injected at 135°C in a precolumn (SHODEX AT-800P from SHOWA DENKO), two mixed-bed columns (SHODEX AT-806 MS from SHOWA DENKO) and one 300-Å μSTYRAGEL column from Waters. The flow rate was 0.8 ml/min. Molecular mass averages and MMDs were determined using the universal calibration curve obtained with narrow MMD polystyrene standards and the following Mark–Houwink parameters for PP in TCB at 135°C: $K = 1.76\,10^{-4}$ and $\alpha = 0.73$ [17]. Data treatment was carried out with Millennium 2010 Chromatography Manager (Waters).

2.2.5. ^{13}C nuclear magnetic resonance analysis of the microstructure of PP fractions

^{13}C NMR analysis was used to characterize the average tacticity in terms of the overall content of meso (*m*) or racemic (*r*) configuration for a given fraction. In this work, the average tacticity was more precisely characterized by the content of meso pentads (*mmmm*%) of TREF fractions of the polypropylenes PP_1 and PP_2 and was determined from the methyl carbon resonance data. From a practical point of view, the content of *mmmm*-pentad sequences is

Table 1
Characterization of non-fractionated polypropylenes PP_1 and PP_2

	Units	PP_1	PP_2
Nucleating agents		no	no
Tacticity percentage (*mmmm*%), as determined by ^{13}C NMR	%	97.2	98.7
Xylene insoluble fraction	wt%	98	99
Flexural elastic modulus[a]	MPa	1680	1850
DMA flexion elastic modulus (E')	MPa	1610	1650

[a] Injection molded samples at 210°C (ISO method 178).

calculated using methyl peaks resonating between 19 and 22 ppm following the relationship:

$$mmmm\% = (S_{mmmm}/S_{\text{total methyl}}) \times 100$$

where S_{mmmm} denotes the area of the *mmmm*-pentad methyl peak at 21.8 ppm and $S_{\text{total methyl}}$ is the sum of the area of all the methyl peaks [18].

300-mg samples were dissolved in 2.5 ml 1,2,4 trichlorobenzene and 0.5 ml hexadeuterobenzene (C_6D_6). ^{13}C NMR spectra were recorded at 130°C on an AMX400 BRUKER spectrometer in pulse Fourier transform (PFT) mode. Experimental conditions were: pulse angle = 90°; sweep width = 220 ppm; relaxation delay = 11 s; time domain = 64 K. All spectra were proton decoupled (inverse gated, Waltz16 pulse scheme).

2.2.6. Atomic force microscopy

Analysis of the rigidity of some key TREF fractions was made possible in this study by means of a quantitative atomic force microscopy method, described elsewhere [19–22]. AFM is particularly well adapted for this study since it can be performed at very small scales, starting from the very low quantity of material that TREF generates, which does not allow the use of classical tools such as DMA to characterize the stiffness of materials.

Samples of some key TREF fractions (60, 80 and 115°C) of the two polypropylenes were prepared as follows. Slices of pellets were taken from the DSC aluminum pans previously used. Thin films, prepared by cutting a thin layer in the pellet, were deposited on to a glass slide. For quantitative analysis of the rigidity, commercial Si_3N_4 cantilevers were used in order to indent the materials. For this purpose, a statistical set of force curves were measured on different areas of the polymer surface. Force curves were obtained by imposing a vertical displacement, z, of the sample toward the tip and by simultaneously measuring the tip displacement, d, through the deflection of the laser beam focused on the cantilever end. The tip–sample interaction force, F, is deduced by means of Hooke's relationship:

$$F = -k_c d \quad (1)$$

where k_c is the stiffness of the cantilever (N/m) given by the manufacturer or experimentally measured.

As largely depicted in the literature [19], force curves are characterized by three different regions depending on the position of the tip during its approach course towards the surface; (i) the "non-contact" region where the tip approaches the surface and is not in contact with the surface, (ii) the "snap-in point" where the tip jumps on to the surface, and, finally, (iii) the electrostatic repulsion region where the tip is in close contact with the surface. In this region, a deflection of the lever can be monitored and increases as the tip–sample interaction force increases. In this work, we only consider the part of the force curve where the electrostatic repulsion forces are dominant.

Since Si_3N_4 tips used in this work are much stiffer than polymers, the tip slightly penetrates the sample surface and an indentation depth δ equal to $z - d$ can be measured. Consequently, all force curves (F vs. z) can be converted into indentation curves (F vs. δ), using the conversion relationship:

$$\delta = z - F/k_c \quad (2)$$

where δ is the indentation depth (nm). For samples with lower elastic modulus, greater indentation depths will be observed.

Making the assumptions that: (i) the indentor is much stiffer than the surface and induces only elastic deformation of the surface, and (ii) that there are negligible adhesion forces between the tip and the surface, the contact between the tip and the surface can be qualified as a static elastic non-adhesive contact. The Hertz mechanical model adapted to the geometry of the tip–sample system can then be used to fit the relationship between F and δ [21,22]. More precisely, a power-law fit is used to characterize the relationship between F and δ:

$$F = AK\delta^n \quad (3)$$

where the exponent n takes different values depending on the geometry of the portion of the tip solicited by the contact; A is a constant defined by all the geometrical parameters of the tip, and K is the elastic constant of the surface.

Knowing the tip geometry, one can easily extract the elasticity constant, K, which is related to Young's modulus E by the relation [21,22]:

$$K = E/(1 - \nu^2) \quad (4)$$

where ν is Poisson's coefficient.

All AFM experiments were carried out with a PicoSPM instrument from Molecular Imaging, operating in ambient atmosphere. Commercial Si_3N_4 0.6-μm microlevers from Park Scientific Instruments were used to indent the surface (triangular-shaped cantilever, wide legs, length = 85 μm, width = 18 μm, thickness = 0.6 μm, stiffness = 0.35 N/m). The tip had a pyramidal shape. From a practical point of view, samples were first imaged by AFM in order to assess the homogeneity of their morphology and the tip

Table 2
Number, weight and z average molecular masses (M_n and M_w, M_z) and polydispersities (H) of non-fractionated polypropylenes PP_1 and PP_2, as determined by SEC

Reference	M_n	M_w	M_z	H
PP_1	77 200	464 600	1 520 000	6.0
	75 500	469 000	1 626 000	6.2
PP_2	57 800	460 100	1 545 000	8.0
	60 600	443 500	1 557 000	7.3

was then positioned on different topographically homogeneous parts of the surface in order to measure force curves.

3. Results and discussion

3.1. Characterization of the non-fractionated materials

The main data concerning the non-fractionated materials are summarized in Table 1. ^{13}C NMR measurements of the isotactic meso pentads (*mmmm*%) have shown that the two polypropylenes PP_1 and PP_2 are highly isotactic polypropylenes with PP_2 having a higher average tacticity (*mmmm*%) than PP_1 (98.7 vs. 97.2%). Consistently, the xylene soluble fraction of PP_2 is lower by about 1% than that of PP_1 (Table 1).

As expected from its larger tacticity, PP_2 has a higher elastic modulus. The flexural elastic moduli of PP_2 and PP_1 were found to be 1850 and 1680 MPa, respectively (Table 1). Further analysis of the mechanical properties realized by means of DMA on the two polypropylenes has confirmed a higher elastic modulus E′ (at 25°C) for PP_2 than for PP_1 ($E' = 1650$ vs. 1610 MPa, respectively). Glass transition temperatures of PP_1 and PP_2 (measured on the tan δ curve, where $\tan\delta = E''/E'$) were 1 and 4°C, respectively. In both cases, results are in good agreement with the fact that PP_2 is characterized by a higher tacticity than PP_1.

Table 2 presents the SEC results for the number (M_n), weight (M_w) and z (M_z) average molecular masses and polydispersity (H) of PP_1 and PP_2. All SEC measurements were replicated twice and are expressed in PP equivalents. As expected, polydispersities of these materials are rather important (from 6.0 to 8.0). It is well known that polyolefins produced with conventional heterogeneous Ziegler–Natta catalysts have broad MMD due to the presence of several types of active site on these catalysts. Polydispersities and molecular mass averages do not change appreciably with polymerization conditions. A slight increase in the polydispersity of homopolymer PP_2 can be detected. This increase is related to a lower M_n value and would then be the indication of the presence of shorter chains in PP_2 than in PP_1.

DSC results on PP_1 and PP_2 are presented in Table 3. A systematically higher crystallization temperature (T_c) and melting temperature (T_m) is observed for PP_2 in comparison to PP_1. The same trend exists for crystallization and melting enthalpies. This clearly indicates a higher ability to crystallize and a higher crystallinity for PP_2 in comparison to PP_1, as the result of its higher tacticity.

This set of data clearly demonstrates that a slight increase of the tacticity of PP_2 polypropylene significantly improves its thermal and mechanical properties. Nevertheless, these average values are not sufficient to completely describe the final mechanical properties of the polymers. A finer understanding of this improvement can be acquired via the determination of the differences of the molecular structure of these two PP which are responsible for the increase of rigidity. More particularly, some information concerning the tacticity distribution of these materials is necessary. This kind of information can be obtained via a TREF fractionation in a wide temperature range (30–130°C) and a characterization of key fractions by ^{13}C NMR, SEC, DSC and AFM.

3.2. Characterization of the fractionated materials

3.2.1. TREF histograms

As depicted in the literature, preparative TREF allows, starting from a few grams of material, the collection of individual fractions, each one containing a set of macromolecules characterized by an identical crystallizability. Fig. 2 shows TREF histograms of PP_1 and PP_2, corresponding to the weight percentage of each fraction vs. the elution temperature ($T_{el.}$). From earlier studies, it has been clearly demonstrated for PP that TREF histograms qualitatively reflect the distribution of isotacticity, with isotacticity increasing almost linearly with the elution temperature [1,9,10]. Fig. 2 shows that both PP_1 and PP_2 are composed of fractions with widely different tacticities, ranging from rather pure atactic ($T_{el.} = 30$°C) to highly isotactic ($T_{el.} = 130$°C). Both polypropylenes are, on the average, highly isotactic since more than 80% of the total fractionated material is eluted above 112°C. As expected from our previous results, significant differences exist between the two resins in the way tacticity is distributed among the chains. A higher

Table 3
Thermal properties of non-fractionated polypropylenes PP_1 and PP_2

Reference	Crystallization temperature (T_c) 1st cooling (°C)	Melting peak temperature (T_m) 2nd heating run (°C)	Crystallization enthalpy (J/g)	Melting enthalpy (J/g)
PP_1	108.8	165.5	98	107
PP_2	110.4	167.8	103	111

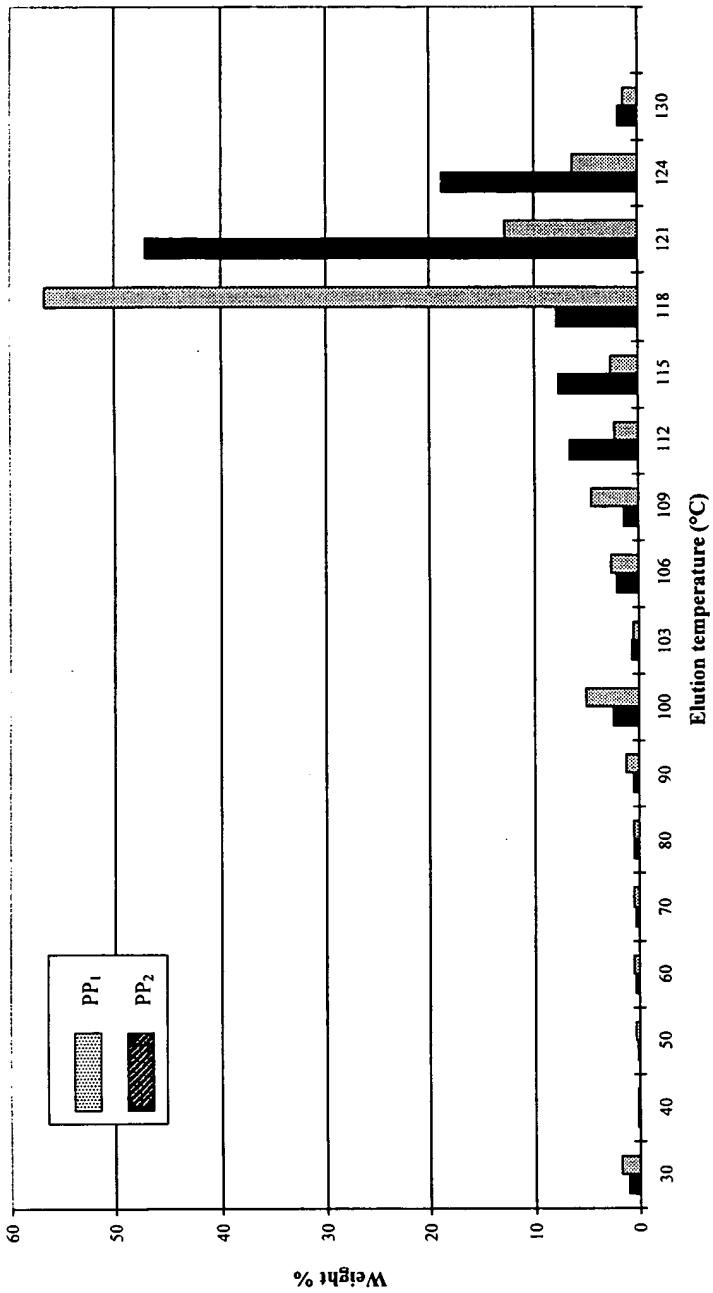

Fig. 2. Superposition of TREF histograms showing the distribution of weight percentage of PP_1 and PP_2 fractions vs. elution temperature (°C).

Table 4
Observed pentad tacticities of selected TREF fractions of PP_1 and PP_2

Reference	Fraction reference (°C)	Percentage of								
		mmmm	*mmmr*	*rmmr*	*mmrr*	*rmrr + mrmm*	*mrmr*	*rrrr*	*mrrr*	*mrrm*
PP_1	60	56.1	10.5	2.5	11.5	3.5	1.6	5.1	3.5	5.7
	100	93.6	2.5	0.0	2.6	0.0	0.0	0.0	0.0	1.2
	112	96.2	1.5	0.0	1.5	0.0	0.0	0.0	0.0	0.7
	118	97.6	0.7	0.2	0.7	0.2	0.2	0.3	0.2	0.0
	121	98.2	0.5	0.2	0.5	0.1	0.2	0.2	0.1	0.0
PP_2	60	66.0	8.9	1.2	9.8	2.7	1.5	5.0	1.2	3.9
	100	95.3	1.9	0.0	2.1	0.0	0.0	0.0	0.0	0.7
	112	98.5	0.6	0.0	0.6	0.0	0.0	0.0	0.0	0.3
	118	98.3	0.9	0.0	0.0	0.0	0.0	0.0	0.0	0.2
	121	100	0.0	0.0	0.0	0.0	0.0	0.0	0.0	0.0

amount of more isotactic fractions is collected for PP_2. This effect is particularly clear when considering the large difference in the proportion of the fractions eluted at 118 and 121°C, respectively, corresponding to the major fractions of PP_1 and PP_2. Indeed, more than 50% of PP_1 is recovered at 118°C, while this occurs at 121°C and even at higher temperatures for PP_2. It must also be noted that the TREF data at 30°C match the results of a classical xylene extraction reported in Table 1. PP_2 is characterized by a lower amount of atactic fraction (1% difference at 30°C). These observations allow us to explain the higher elastic modulus E measured for PP_2, resulting from the different polymerization conditions used to produce this polymer.

3.2.2. ^{13}C NMR analysis of the fractions

Some key fractions of polypropylenes PP_1 and PP_2 were analyzed by ^{13}C NMR in order to evaluate pentad isotacticity, according to the procedure described above. Table 4 presents pentad isotacticities of the fractions of PP_1 and PP_2 eluted at 60, 100, 112, 118 and 121°C.

As expected, isotacticity of the fractions increases with the elution temperature, confirming that the TREF of polypropylenes is mainly conducted on the basis of tacticity. However, an interesting outcome of this analysis is that the isotacticities of PP_2 fractions are systematically larger than those of PP_1 fractions, at a given elution temperature. This is illustrated by Fig. 3, which shows the evolution of *mmmm*% pentads for some fractions of PP_1 and PP_2 as a function of elution temperature. The tacticity is different between fractions of PP_1 and PP_2 eluted at the same given temperature, thus presenting the same crystallizability. Larger differences are observed for the fractions collected at low elution temperature. This indicates that, contrary to what is sometimes implicitly assumed, TREF does not strictly fractionate polyolefins as a function of chain tacticity. In fact, it separates chains according to their ability to enter in a crystal having a thickness determined by the temperature during crystallization. Consequently, only one regular sequence of sufficient length is required to bring a chain in a given TREF fraction [23]. Depending on whether the rest of the chain

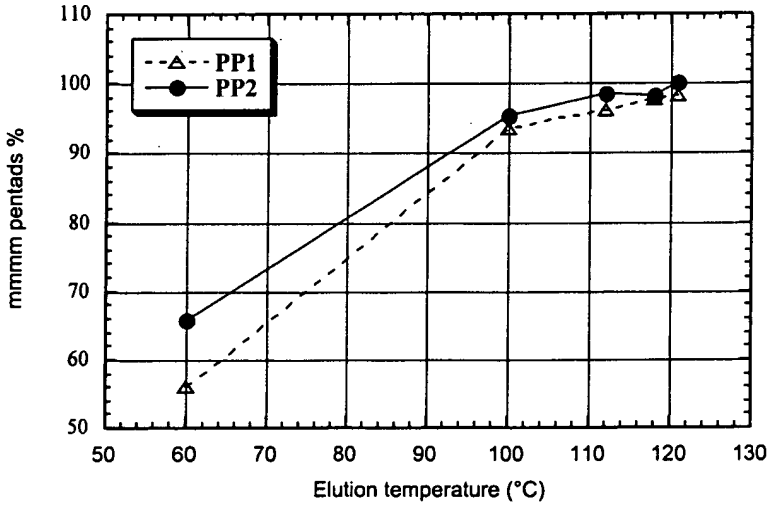

Fig. 3. Meso pentads percentage (*mmmm*%) of PP_1 and PP_2 fractions versus TREF elution temperature.

Table 5
Number, weight and z average molecular masses (M_n, M_w and M_z) and polydispersity (H) of PP_1 and PP_2 TREF fractions, as determined by SEC analysis

Reference	TREF elution temperature (°C)	M_n	M_w	M_z	H
PP_1	30	19 500	199 200	1 002 000	10.2
	90	18 100	84 200	371 000	4.6
	100	29 900	86 100	237 000	2.9
	103	22 700	77 900	241 000	3.4
	106	36 100	93 300	238 000	2.6
	109	51 100	117 200	280 000	2.3
	112	43 200	101 900	216 000	2.4
	115	58 800	131 100	311 000	2.2
	118	85 500	437 400	128 000	5.1
	121	220 300	779 700	2 017 000	3.5
	124	247 400	848 900	2 333 000	3.4
PP_2	30	18 100	84 200	393 000	4.6
	100	18 100	43 700	108 000	2.4
	103	15 900	52 900	190 000	3.3
	106	27 900	74 300	237 000	2.7
	109	23 200	59 700	142 000	2.6
	112	45 500	91 900	173 000	2.0
	115	60 700	121 900	221 000	2.0
	118	67 200	150 400	282 000	2.2
	121	172 300	482 700	1 235 000	2.8
	124	293 000	913 300	2 200 000	3.1

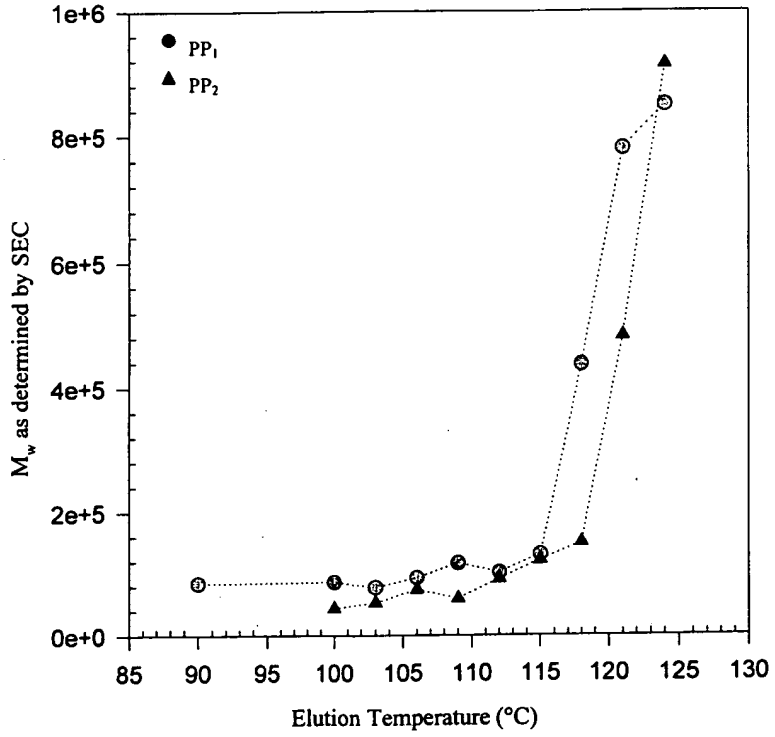

Fig. 4. Evolution of the weight average molecular mass (M_w) of key TREF fractions of PP_1 and PP_2 vs. elution temperature.

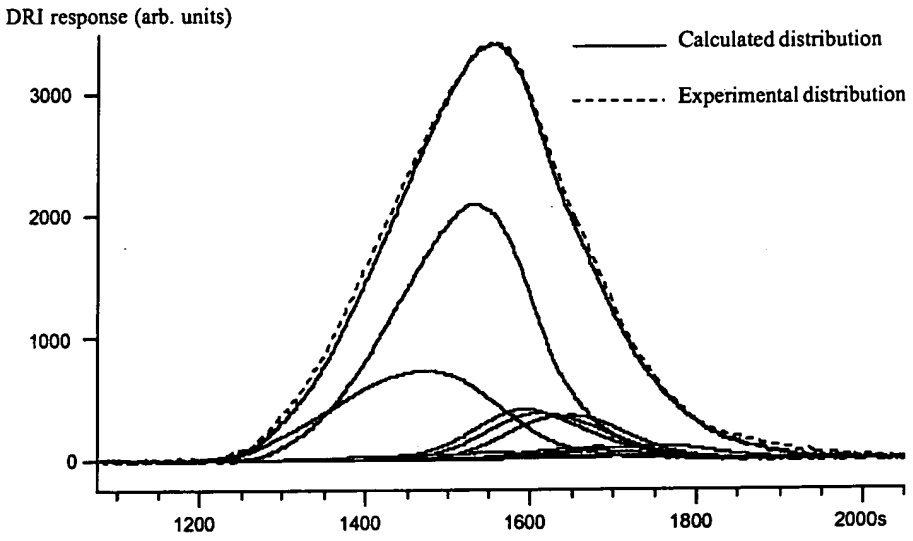

Fig. 5. Superposition of the SEC chromatograms of each PP_2 TREF fraction. Comparison between the initial broad distribution of the non-fractionated polypropylene (dashed line) and the calculated distribution (solid line) obtained from the superposition of the weighted chromatograms of the TREF fractions.

consists of regular sequences of similar or shorter lengths, the average tacticity of the fraction will be larger or smaller.

3.2.3. SEC analysis of the fractions

The mass averages and MMD of some key polypropylene fractions are displayed in Table 5. Fig. 4 describes the evolution of the weight average molecular mass (M_w) of key TREF fractions of PP_1 and PP_2 with respect to the TREF elution temperature.

Interestingly, the polydispersity H of each fraction (except the first one) is significantly lower than that of the non-fractionated material (Tables 1 and 5). This reduction is a further indication of the influence of the catalyst. Polypropylenes produced with conventional heterogeneous Ziegler–Natta catalysts are characterized by broad MMDs, ranging from 4 to 12 and arising from the presence of several types of sites on these catalysts. Some authors report that these distributions can be adequately described as superpositions of a series of narrower distributions, one for each type of catalytic site, with each site type producing a Flory's most probable chain-length distribution around 2 [6]. In this work, the reduction of polydispersity observed for TREF fractions of PP_1 and PP_2 might reasonably be attributed to the ability of TREF to isolate different fractions originating from different site types.

In a related way, the superposition of the distributions of each fraction is expected to yield back the initial broad MMD of the non-fractionated polypropylenes if properly normalized by the weight content of the fraction in the resins. This is illustrated in Fig. 5 for PP_2 where it can be seen that experimental and recalculated curves superimpose completely, a clear indication that the fractionations are quantitative.

From the data obtained by ^{13}C NMR and SEC characterization of the TREF fractions, it is also interesting to point out the following information:

- One observes a dramatic increase of M_w above $T_{el.}$ = 115°C. This illustrates the way catalysis orientates tacticity as a function of the different molecular masses of PP_1 and PP_2, reflecting the inter-molecular heterogeneity. More precisely, it appears from Fig. 4 that Ziegler–Natta catalysts insert preferably the stereodefects in the shortest chains, since low molecular mass fractions are collected at low elution temperatures. Similarly, longer isotactic sequences are recovered in fractions of higher masses, eluted at higher elution temperatures.
- Closer inspection of Fig. 4 reveals, however, significant differences between PP_1 and PP_2. The curve representative of PP_2 is slightly shifted to a higher elution temperature compared to that of PP_1. For a given elution temperature (given crystallizability), M_w is systematically lower for PP_2 than for PP_1. This effect is prominent for fractions collected at 118 and 121°C, at which temperatures the difference in M_w reaches 300 000 between PP_1 and PP_2. Shorter chains of PP_2 have thus the same crystallizability than longer chains of PP_1. This behavior reflects the effect of specific catalytic systems used to polymerize PP_1 and PP_2 leading to different distributions of tacticity as a function of the molecular masses. In other words, PP_1 and PP_2 do not have the same inter-molecular heterogeneity.
- The stronger variations of tacticity detected by ^{13}C NMR between fractions of PP_1 and PP_2 seem to concern those fractions that are characterized by lower molecular masses, collected in the low temperature range. However, in this elution temperature range, the observed

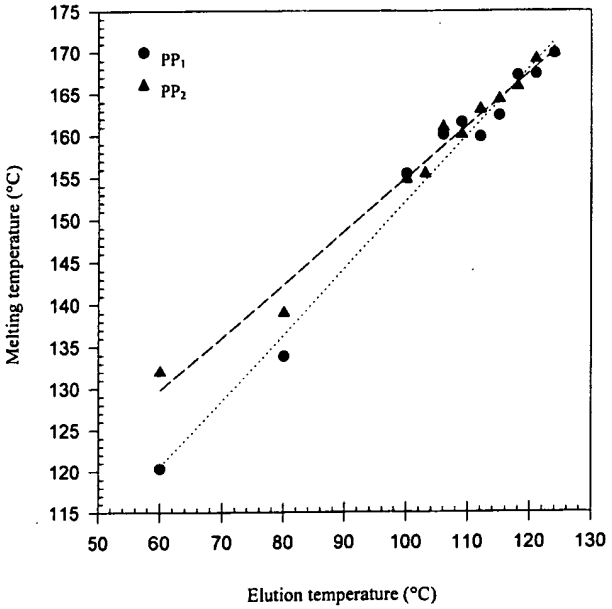

Fig. 6. Evolution of melting temperatures (T_m) of key TREF fractions of PP_1 and PP_2 versus TREF elution temperature.

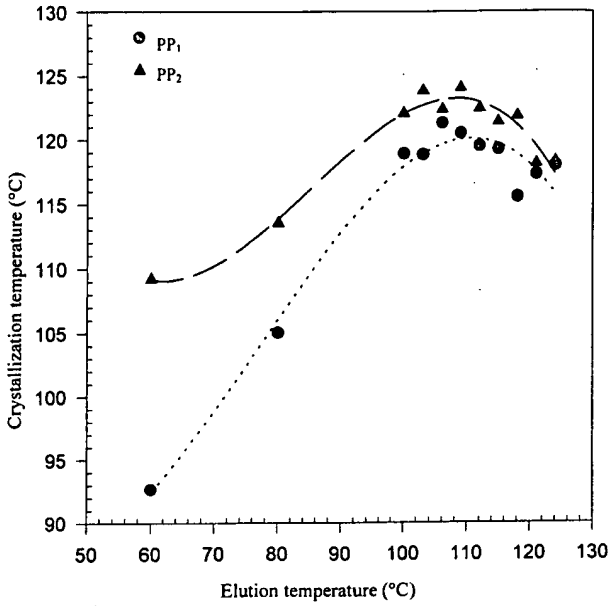

Fig. 8. Evolution of crystallization temperatures (T_c) of key TREF fractions of PP_1 and PP_2 versus TREF elution temperature.

trend is that differences between the molecular masses of PP_1 and PP_2 fractions are much less important than for higher elution temperature. For instance, fractions of PP_1 and PP_2 collected at 112°C have the same molecular mass. Under these conditions, variations of tacticity detected are believed to reflect a change of the intra-molecular distribution of tacticity. Therefore, we may certainly conclude that the intra-molecular distribution of tacticity is broader for PP_1. This suggests that the Ziegler–Natta catalysis also seems to influence the intra-molecular heterogeneity and that the modification of this catalysis for the polymerization of PP_1 and PP_2 would be capable of inducing changes in their intra-molecular heterogeneity.

To summarize, all the data obtained up to now with the TREF fractions lead to explain mainly, the difference of rigidity observed for the two PP on the basis of a stronger shift of the tacticity distribution of two fractions of PP_1 and PP_2: fraction collected at 118°C for PP_1 and fraction collected at 121°C for PP_2, which are, respectively, the major fractions of PP_1 and PP_2 (Figs. 2 and 3, Table 4).

3.2.4. Thermal analysis of the fractions

Fig. 6 presents the evolution of melting temperatures (T_m) for PP_1 and PP_2 fractions as a function of elution temperature. A quasi linear evolution of T_m with elution temperature is observed for both resins. This clearly demonstrates that lamellar thicknesses, corresponding to the fractions

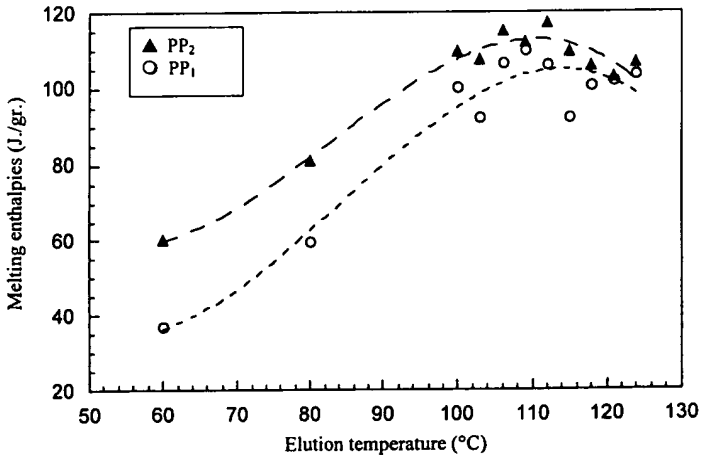

Fig. 7. Evolution of melting enthalpies of PP_1 and PP_2 TREF fractions versus TREF elution temperature.

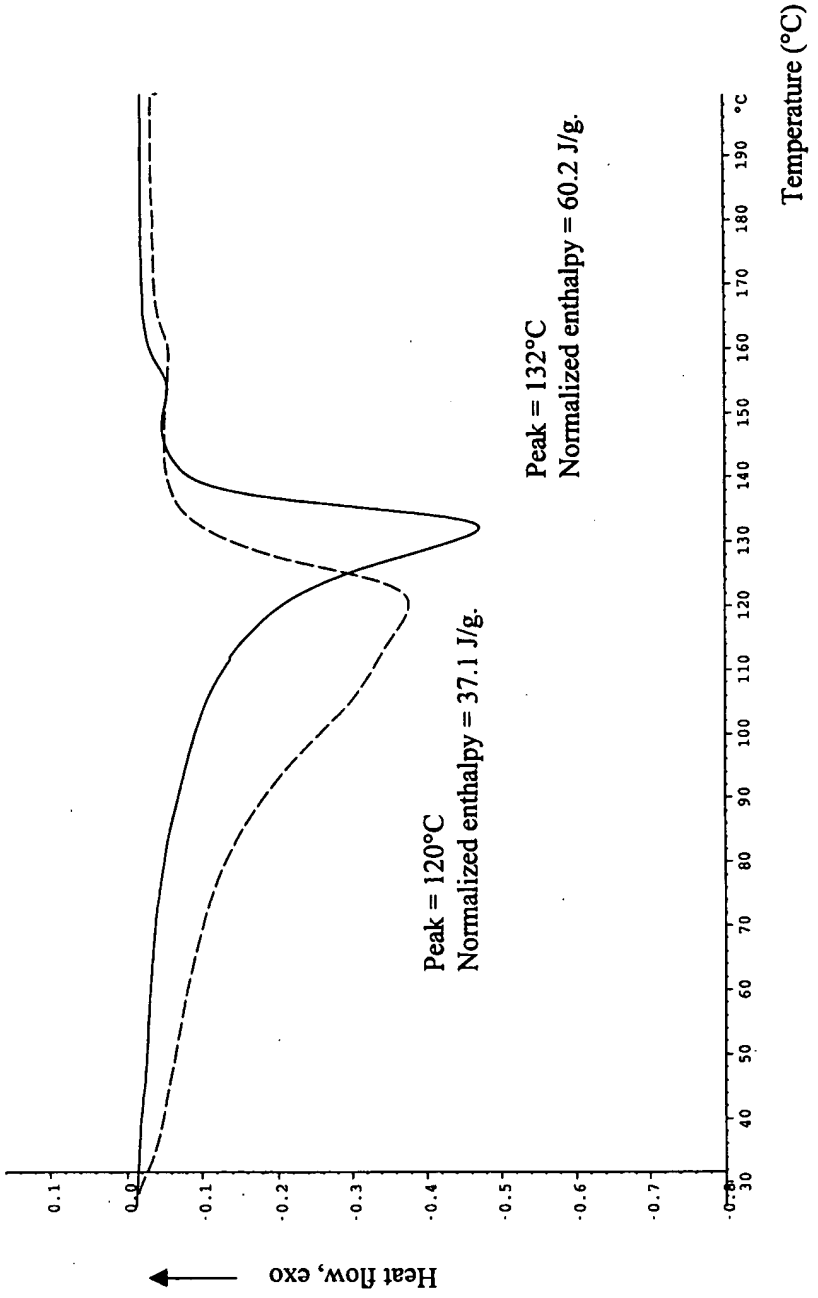

Fig. 9. Melting DSC thermograms of PP_1 (dashed line) and PP_2 (solid line) TREF fractions eluted at 60°C.

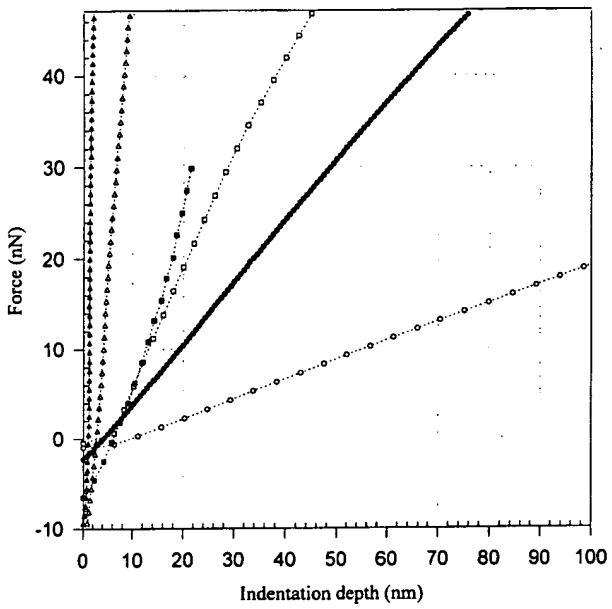

Fig. 10. Typical force–indentation curves measured on key TREF fractions of PP_1 (O-□-Δ) and PP_2 (●-■-▲), respectively, collected at 60, 80 and 115°C.

crystallized in given conditions, increase as a function of elution temperature (or molar mass) for the two polymers, which is another clear indication of the inter-molecular heterogeneity.

However, slight differences between T_m of PP_1 and PP_2 fractions can be detected for fractions eluted at low temperatures: in this temperature range (60–90°C), PP_2 fractions are characterized by higher T_ms than PP_1 fractions. These PP_2 fractions are thus characterized on the average by longer crystallizable sequences than equivalent fractions of PP_1. These results are in good agreement with the tacticity data obtained by ^{13}C NMR.

Melting enthalpies of TREF fractions of PP_1 and PP_2 fully confirm these conclusions (Fig. 7). PP_2 TREF fractions are characterized by a systematically higher crystallinity than PP_1 TREF fractions, owing to the higher tacticity percentage of PP_2 fractions. If we now consider crystallization temperature (T_c), the differences between the corresponding fractions of PP_1 and PP_2 are maintained (Fig. 8), indicating that T_c is also mainly dependent on isotacticity. Nevertheless, a slight decrease in T_c is observed for the last TREF fractions of each sample. This is most probably caused by the restricted mobility of very long chains in these fractions (Fig. 4).

Hence, all thermal results converge in supporting the previous observation that PP_1 fractions are of lower tacticity than PP_2 fractions eluted at the same temperature. Clearly, the distribution of lengths of regular isotactic sequences within the same chain is more heterogeneous for PP_1 than for PP_2. A supplementary illustration of this broader intramolecular heterogeneity is given in Fig. 9, where the melting endotherms of fractions of PP_1 and PP_2 eluted at 60°C are compared. The broader endotherm of PP_1 testifies of a broader distribution of isotactic sequence lengths in PP_1.

3.2.5. Analysis of the TREF fractions by means of AFM

Typical indentation curves of some key TREF fractions of the two polypropylenes, collected at 60, 80 and 115°C, are presented in Fig. 10. As mentioned in the experimental part, the slope of these indentation curves increases with the elastic modulus of the sample.

Based on this, it appears from Fig. 10 that the elastic modulus increases with elution temperature; i.e. with the tacticity and the crystallinity of the fractions (see DSC and ^{13}C NMR results). Moreover, at constant elution temperature, elastic moduli of PP_2 TREF fractions are found to be systematically higher than those of PP_1 TREF fractions. For each TREF fraction, the force was found to

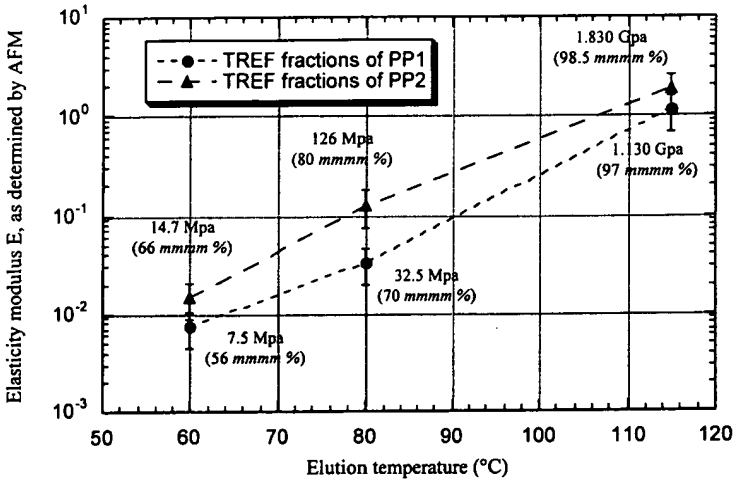

Fig. 11. Evolution of the elastic modulus of PP_1 and PP_2 TREF fractions, calculated from the AFM force–indentation curves, versus elution temperature. Circles: PP_1, triangle: PP_2.

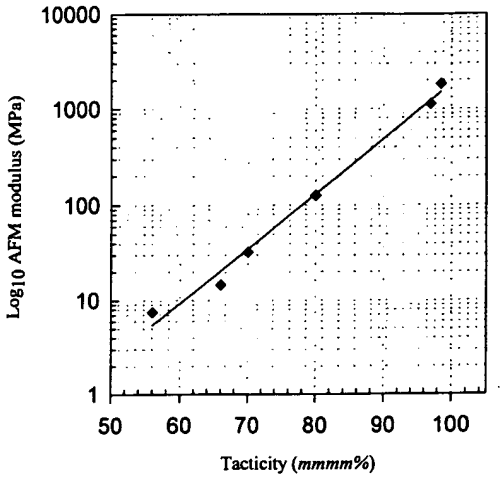

Fig. 12. Evolution of the logarithm of the elastic modulus of PP_1 and PP_2 TREF fractions, calculated from the AFM force–indentation curves, versus the tacticity.

vary with the indentation depth following a power-law relationship with the exponent $n = 3/2$. This suggests that the force–indentation curves can be modeled with the Hertz mechanical model using a spherical or a paraboloid punch geometry [21], following the equations:

$$F = \tfrac{4}{3}\sqrt{R}K\delta^{3/2} \quad (5)$$

$$F = \tfrac{4}{3}\sqrt{2k}K\delta^{3/2} \quad (6)$$

where R is the radius of the spherical tip apex and k is the coefficient characterizing the tip paraboloid profile.

Using the spherical equation for the small indentation depth with $R = 40$ nm and the paraboloid equation for larger indentation depths with $k = 14$ nm, the elastic constant, K, was deduced for each TREF fraction. This was carried out by fitting a statistical set of indentation curves and, for each curve, by fitting different portions of the repulsion region and taking the average value. The tensile modulus, E, was then calculated from Eq. (4) using a value of 0.3 for Poisson's ratio, which is valuable for stiff samples.

In Fig. 11, the obtained values of E are reported as a function of the elution temperature. For each TREF fraction, *mmmm*% measured by ^{13}C NMR, is also indicated. For both PP_1 and PP_2, Fig. 11 clearly shows a strong increase of the modulus versus the elution temperature. This evolution spans over two orders of magnitude and demonstrates that differences in tacticity have a strong impact on the elastic properties. The larger elastic modulus of PP_2 fractions, resulting from the narrower intra-molecular distribution of regular sequence lengths, is clearly detected on these curves.

In Fig. 12, the logarithm of the elastic modulus of PP_1 and PP_2 TREF fractions is plotted *versus* the tacticity of these fractions. One can observe that the modulus of the fractions varies exponentially with their tacticity, confirming that a weak modification of the tacticity fundamentally modifies the chain crystallizability and, thus, the rigidity of the polymer.

In Fig. 13, the elastic modulus of PP_1 and PP_2 TREF fractions is presented as a function of their corresponding crystallization enthalpies. The observed relationship is fairly well fitted by an exponential law. This reveals that very small differences in crystallinity can strongly affect the elastic modulus, as expected from simple mechanical models, due to the huge difference between the elastic moduli of crystalline and amorphous regions.

These results show that the difference in the average rigidity measured for the two polypropylenes can be understood as a consequence of the different rigidities of different constitutive fractions of the materials. TREF thus allows us to understand the complexity of the materials in terms of the different rigidities that heterogeneous Ziegler–Natta catalysts can generate.

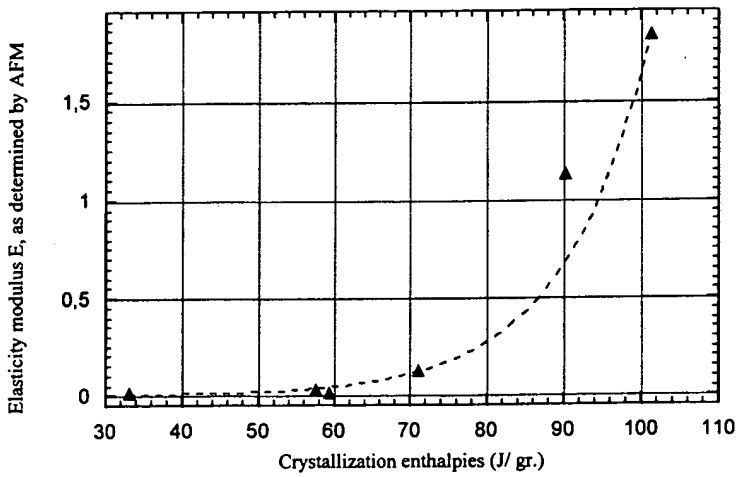

Fig. 13. Evolution of the elastic modulus of PP_1 and PP_2 TREF fractions, as determined by AFM, versus crystallization enthalpies of the fractions.

4. Conclusions

Two different polypropylenes, PP_1 and PP_2, synthesized with heterogeneous Ziegler–Natta catalysts, were studied in this work. Polymerization conditions were adapted in order to produce a polymer PP_2 characterized by a higher stiffness than polymer PP_1.

First results acquired on the non-fractionated materials have confirmed that PP_2 was characterized by a higher crystallinity and elastic modulus, in good agreement with its higher tacticity. Based on this, we focused our attention on the determination of the molecular structure parameters of these two polymers conditioning their rigidity. To achieve this goal, a preparative temperature rising elution fractionation (TREF) of both resins was realized and the analysis of the fractions was carried out by means of ^{13}C NMR, SEC and DSC. The slight differences detected between the original resins were detailed in a much better way by considering these TREF fractions.

On the one hand, comparison between the two TREF histograms revealed significant differences between the two PP. Indeed, a higher weight percentage of more crystalline fractions was recovered for polypropylene PP_2, which allows us to explain the higher elastic modulus observed for this polymer.

On the other hand, fractionation of both resins by TREF allowed us to understand the observed differences in terms of varying properties of the constituent fractions. It was found that the differences between the two resins originate primarily from subtle variations in the way tacticity is distributed between the chains.

^{13}C NMR analysis of the fractions has first clearly shown that TREF fractions of PP_2 were more isotactic than for PP_1 at a given elution temperature. This result not only allows us to explain the difference of rigidity observed between the two resins, but is also a clear indication that TREF does not strictly fractionate polypropylenes according to tacticity. Instead, recent numeric simulation has shown that TREF fractionates PP according to the longest crystallizable sequence in a chain [23].

^{13}C NMR and SEC data of the TREF fractions have shown that Ziegler–Natta catalysts used in this work insert preferably the stereodefects on the low molecular masses of polypropylene. It has also revealed that the distribution of the tacticity is a function of the different molecular masses was different between the two PP, which means a change of the inter-molecular heterogeneity. More precisely, adaptation of the polymerization conditions were here found to shift the distribution of tacticity to lower molecular masses in the case of polypropylene PP_2, leading to a decrease of tacticity defects on low molecular mass fractions for this polymer. Thermal analysis of the fractions by means of DSC brought a further confirmation of this modification of the inter-molecular heterogeneity.

In addition, a comparative study of the fractions by SEC, DSC and ^{13}C NMR also seems to reveal a different intra-molecular distribution of tacticity between PP_1 and PP_2, which means a different intra-molecular heterogeneity. More precisely, it seems in this case that the intra-molecular heterogeneity is broader for PP_1 with, as a consequence, a lower average tacticity for PP_1 fractions than for PP_2 fractions for a given elution temperature. Although this is not an unexpected result, it has not been, to the best of our knowledge, experimentally demonstrated so far.

Obviously, such a difference may be responsible for differences in mechanical properties between the resins. This has been illustrated by measuring the elastic moduli of key TREF fractions of PP_1 and PP_2 by AFM for the first time. It was found that elastic moduli of key TREF fractions of both polypropylenes evolve over two orders of magnitude with respect to the elution temperature and vary very strongly with the crystallinity and the tacticity of the fractions. Moreover, TREF fractions of PP_2 were found to exhibit a systematically higher elastic modulus than PP_1 TREF fractions, in good agreement with their higher average tacticity. Based on this, the larger average elastic modulus measured on non-fractionated PP_2 can be understood as a combination of the different rigidities of the different constituent fractions generated by the catalyst.

It should be noted here that a similar work has been realized for two PP/EP resins synthesized in the same polymerization conditions. This last work mainly deals with the characterization of the molecular structure of the corresponding EP copolymer phase through a TREF fractionation coupled with the analysis of the fractions by means of FTIR and DSC. A correlation is made with the results presented here. These results will be published in the near future.

Acknowledgements

The authors gratefully acknowledge M.L. LAMOTTE for NMR measurement (FINA RESEARCH) and "La Région Wallonne" for the financial support.

References

[1] Soares JBP, et al. Polymer 1996;37(20):4607–13.
[2] Soares JBP, et al. Ind Engng Chem Res 1997;36:1144–50.
[3] Goodall BL. In: Van der Ven S, editor. Polypropylene and other polyolefins: polymerization and characterization, Studies in Polymer Science, vol. 7. Amsterdam: Elsevier, 1990. p. 1–13.
[4] Mani R, et al. TRIPS 1993;1(10):322–8.
[5] Mirabella, et al. J Polym Sci Part B Polym Phys 1994;32(12):1205–16.
[6] Soares JBP, et al. Polymer 1996;37(20):4595–605.
[7] Yomada K, et al. Polymer 1998;39(22):5327–33.
[8] Xu J, et al. J Appl Polym Sci 1996;62:727–31.
[9] Xu J, et al. Eur Polym J 1998;34(3/4):431÷4.
[10] Kioka M, et al. Polymer 1994;35(3):580–3.
[11] Paukkeri R, et al. Polymer 1994;35(12):2636–43.
[12] Paukkeri R, et al. Polymer 1994;35(8):1673–9.
[13] Lehtinen A, et al. Macromol Chem Phys 1994;195:1539–56.

[14] Paukkeri R, et al. Polymer 1993;34(12):2488–94.
[15] Soares JBP, et al. Polymer 1995;36(8):1639–54.
[16] Mizuno A, et al. J Appl Polym Sci Appl Polym Symp 1993;52:159–72.
[17] Halmers et al., IUPAC, 1976.
[18] Ray GJ, et al. Macromolecules 1977;10(4):773–8.
[19] Burnham NA, et al. In: Bonnell DA, et al., editors. Scanning tunneling microscopy and spectroscopy theory, techniques and applications. New York: Springer, 1993. p. 191–250.
[20] Burnham NA, et al. Nanotechnology 1993;4:64–80.
[21] Sneddon IN. Int J Engng Sci 1969;3:47–57.
[22] Tomasetti E, et al. Nanotechnology 1998;9:305–15.
[23] Lodefier Ph, et al. Macromolecules 1999;32:7135–9.